ALICE Pb-Pb and p-Pb results*

Dariusz Miśkowiec

GSI Darmstadt

for the ALICE Collaboration

I present here a selection of results reported by the ALICE experiment during the first three years of the LHC operation. The emphasis is on the soft observables and on the first data from the p–Pb collisions collected in a short pilot run in September 2012.

PACS numbers: 25.75.-q, 24.85.+p

1. Introduction

ALICE (A Large Ion Collider Experiment) is an experiment at the Large Hadron Collider (LHC) dedicated to studies of QCD matter created in energetic collisions between lead nuclei [1]. QCD predicts that at energy densities above 1 GeV/fm^3 a state of deconfined quarks and gluons occurs, possibly accompanied by chiral symmetry restoration in which quarks assume their current masses. The QCD matter can be probed using high-p_{T} particles and heavy flavors. Assessing its properties in detail, however, requires good understanding of the underlying collision dynamics which can be best studied via the bulk particle production observables like the transverse momentum spectra of light flavors, flow, fluctuations, and femtoscopy.

ALICE has a high granularity, a low transverse momentum threshold $p_{\mathrm{T}}^{\mathrm{min}} \approx 0.15$ GeV/c, and a good hadron identification up to several GeV/c. The setup is shown in Fig. 1. The central-barrel detectors, the Inner Tracking System (ITS), the Time Projection Chamber (TPC), the Transition Radiation Detector (TRD), and the Time Of Flight (TOF), cover the full azimuthal angle range at midrapidity $|\eta| < 0.9$. The calorimeters EMCal and PHOS and the particle identification detector HMPID have partial coverage at midrapidity. The V0 detector measures charged-particle multiplicity at $-3.7 < \eta < -1.7$ and $2.8 < \eta < 5.1$ and is mainly used for

* Presented at the Cracow Epiphany Conference in January 2013.

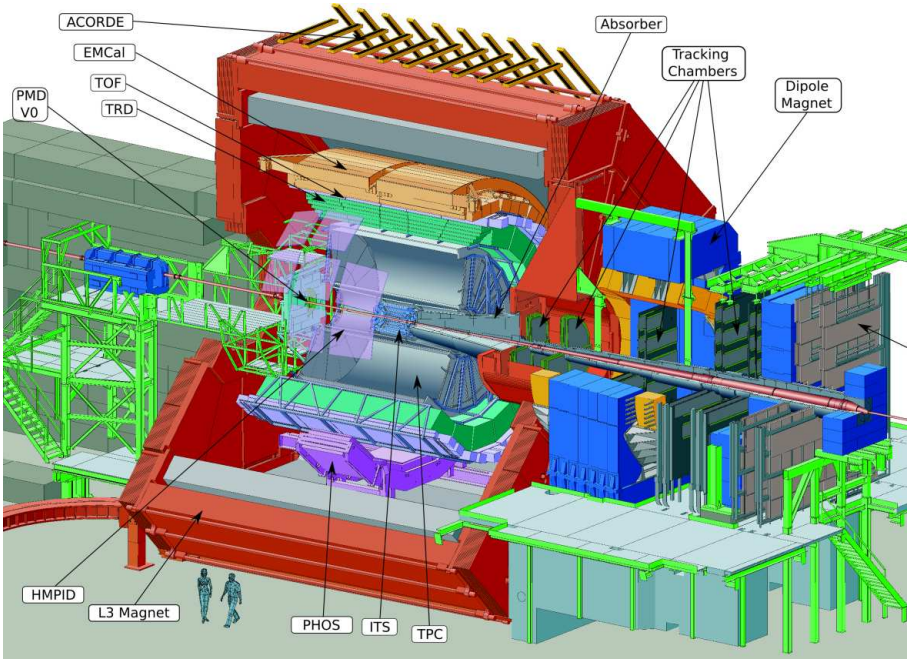

Fig. 1. The ALICE experiment at the CERN LHC. The central-barrel detectors (ITS, TPC, TRD, TOF), with a pseudorapidity coverage $|\eta| < 0.9$, address the particle production at midrapidity. The centrality is derived from the charged-particle multiplicity at $-3.7 < \eta < -1.7$ and $2.8 < \eta < 5.1$.

triggering and centrality determination. The complete list of ALICE detectors and their detailed description can be found in Ref. [1]. The data sets so far collected by ALICE are summarized in Table 1.

Table 1. Data sets collected by ALICE in 2009–2012. In pp running, the interaction rate at ALICE was reduced by displacing the beams or using satellite bunches. The short p–Pb run in 2012 listed here was followed by 6 weeks in 2013.

system	$\sqrt{s_{\mathrm{NN}}}$ (TeV)	running time
pp	0.9, 2.36, 2.76, 7.0, 8.0	3 years
Pb–Pb	2.76	8 weeks
p–Pb	5.02	8 hours

2. Particle production

The bulk particle production is a basic indicator of entropy during a nuclear collision. The charged-particle pseudorapidity density in central (0-5%) Pb–Pb collisions at $\sqrt{s_{\rm NN}}$ =2.76 TeV, normalized to the number of participants, is $\mathrm{d}N_{\rm ch}/\mathrm{d}\eta/\langle N_{\rm part}\rangle \approx 4$, about two times higher than in pp collisions at the same energy, and also about twice as high as in the gold–gold collisions at RHIC (Fig. 2). Both in pp and Pb–Pb the charged-particle pseudorapidity density is a power-law function of $\sqrt{s}$. The exponent is higher in nuclear collisions. The observed charged-particle pseudorapidity density exceeds the predictions of most models with the initial state gluon saturation. The particle yield from p–Pb, once normalized to the number of participating nucleons, falls on the inelastic pp collision curve. The bulk particle production was subject of the first ALICE (and LHC) publications from the pp [3, 4], Pb–Pb [5], and p–Pb [2] campaigns at the LHC. The measured yields define the entropy and thus set the stage for the hydrodynamical modeling of heavy-ion collisions.

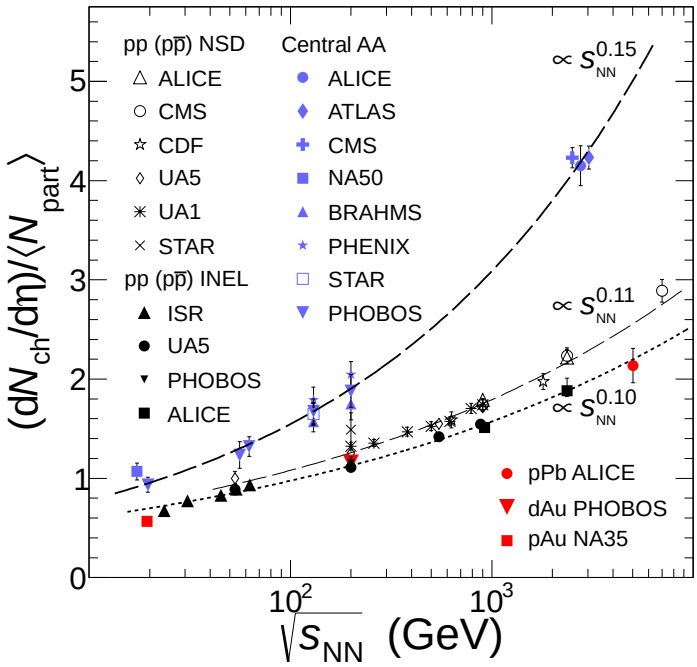

Fig. 2. Charged-particle production at midrapidity from pp, p–Pb, and Pb–Pb collisions (from Ref. [2]). Particle yield per participant in Pb–Pb at the LHC is about two times higher than in pp. It is also more than twice as high as in Au–Au at RHIC. The p–Pb measurement coincides with the inelastic pp curve.

While the pseudorapidity distributions of particles produced in pp and Pb–Pb are essential to understand the dynamics of heavy-ion collisions, the analogous distribution in p–Pb constrains its initial conditions. Figure 3 compares the distribution measured by ALICE with several models [2]. Models which include shadowing or saturation agree with the measurement within 20%. The saturation models predict a too steep η dependence. Vacuum models clearly overshoot the measurement.

Additional information is contained in the centrality dependence of the charged-particle pseudorapidity density. The centrality of the collision events was derived from the charged-particle multiplicity seen in the V0 detector at $-3.7 < \eta < -1.7$ and $2.8 < \eta < 5.1$ as described in Ref. [6]. The number of participants and the number of binary collisions, $N_{\rm part}$ and $N_{\rm coll}$, were calculated for each impact parameter using Glauber model. The centrality resolution was better than 1%.

The centrality dependence of the normalized charged-particle pseudorapidity density turns out to coincide in shape with the one measured at RHIC (Fig. 4). This is against the expectation that an increased contribution of hard processes should lead to a steeper centrality dependence at the LHC.

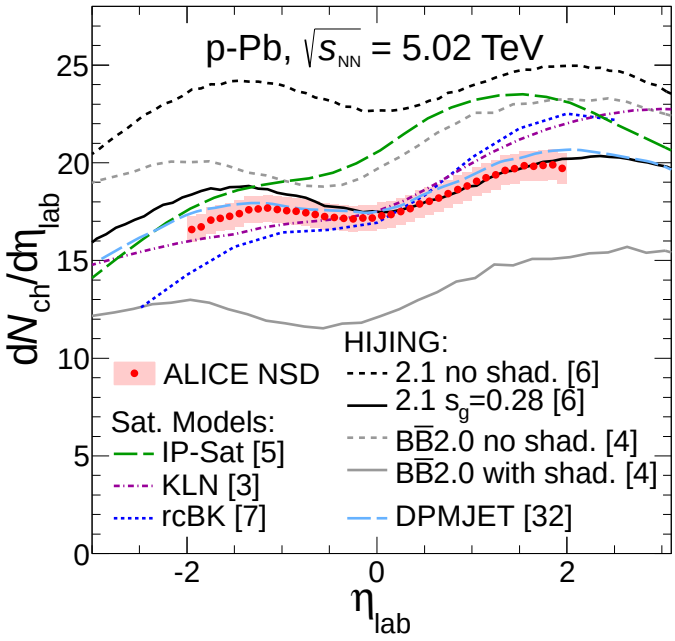

Fig. 3. ALICE $\mathrm{d}N_{\rm ch}/\mathrm{d}\eta$ in p–Pb, compared to models. Models with shadowing or saturation agree with the measurement within 20%. The citation numbers in the plot refer to Ref. [2] from which this figure was taken.

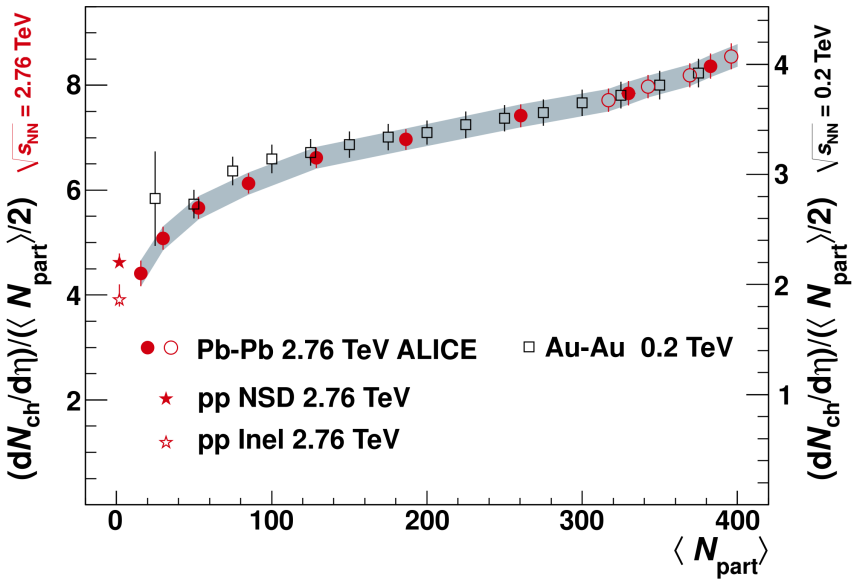

Fig. 4. Charged-particle production as a function of centrality (from Ref. [7]). The LHC measurement coincides with the scaled RHIC data.

The weak centrality dependence observed is presumably related to the nuclear shadowing and is, in fact, reasonably well reproduced by models which take this phenomenon into account [8].

3. Identified hadrons

The description of the reaction dynamics can be strongly constrained using measurements of identified hadrons. The central barrel of ALICE ($|\eta| < 0.9$) has good particle identification capability. Transverse momentum spectra of pions, kaons, and protons from central Pb–Pb collisions [9] are shown in Fig. 5. The spectra at the LHC are harder than at RHIC [10]. A blast wave fit allows one to associate this fact with a 10% increase of the average transverse flow velocity (Fig. 6).

Hydrodynamic predictions [11] underestimate the pion and kaon yields at high-p_{T} (dotted cyan line in Fig. 5). On the other hand, they significantly overestimate proton yield which might indicate a too high chemical freeze-out temperature T_{ch}. A similar discrepancy is present in the thermal model. There, however, a lower T_{ch} is excluded by the Ξ and Ω yields [12]. The details of the identified hadron analysis are given in Ref. [9].

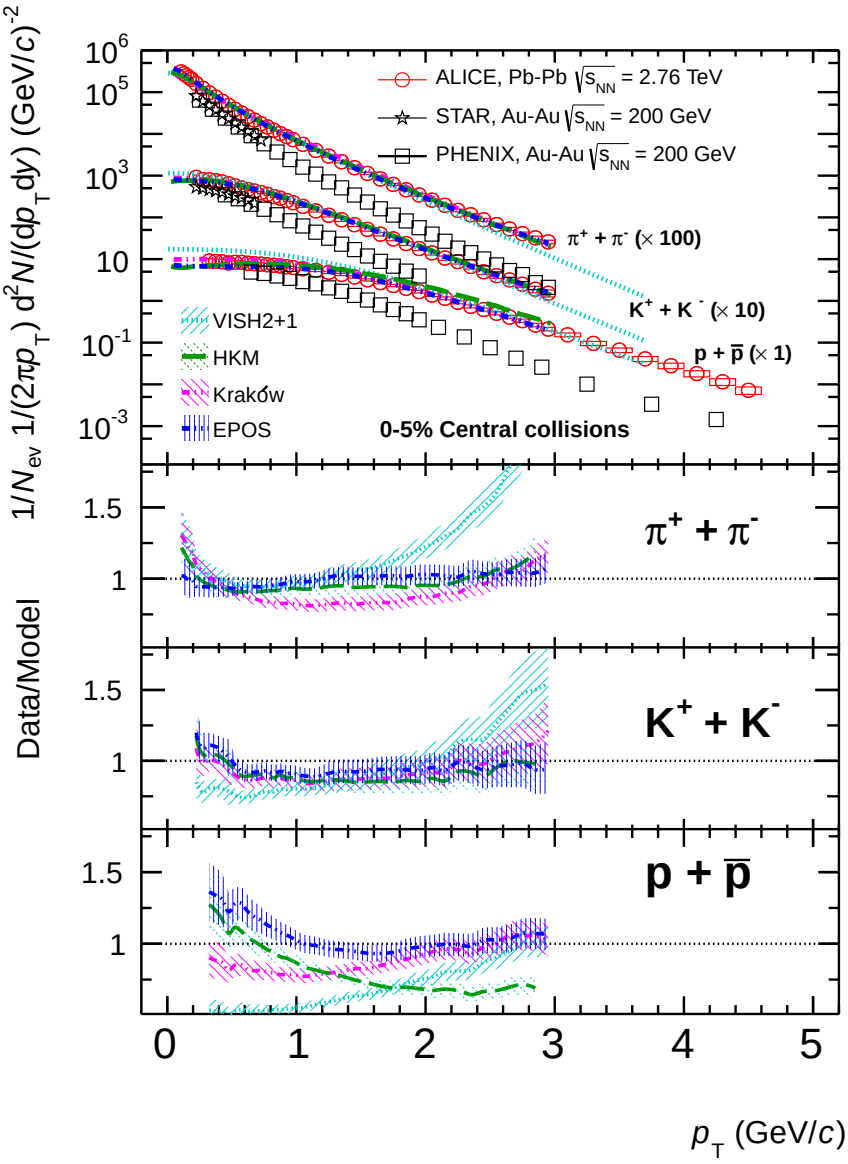

Fig. 5. Transverse momentum spectra of identified hadrons in central Pb–Pb collisions from ALICE, compared to RHIC data and to model calculations (from Ref. [9]).

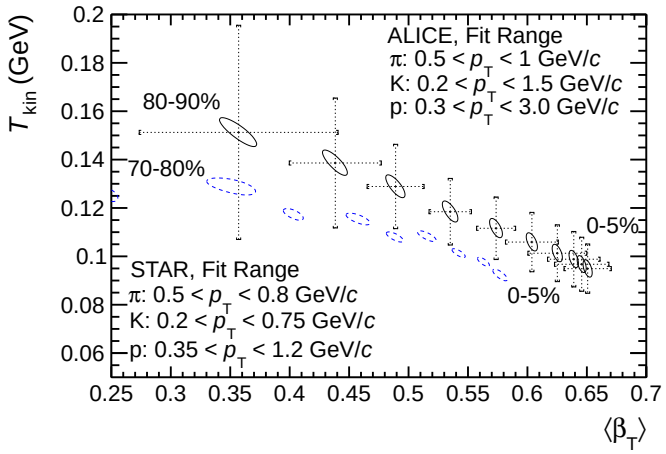

Fig. 6. Temperature and collective velocity extracted from the blast-wave fit to transverse momentum spectra of pions, kaons, and protons in Pb–Pb collisions of various centralities (from Ref. [9]). The mean collective transverse velocity at LHC is 10% higher than at RHIC.

4. Femtoscopy

Spatial extension of the source of pions with a fixed momentum vector (homogeneity length, or Hanbury Brown–Twiss (HBT) radius) is accessible via the Bose-Einstein correlations aka HBT analysis. The pion homogeneity volume measured by ALICE in most central 5% Pb–Pb collisions at $\sqrt{s_{\rm NN}}$ =2.76 TeV [13] is shown in Fig. 7. The volume is about two times larger than

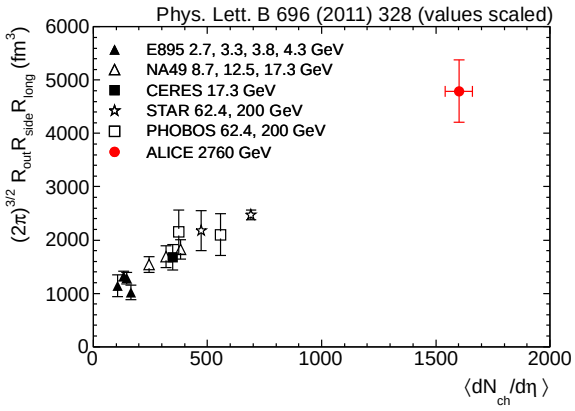

Fig. 7. Homogeneity volume in central gold and lead collisions at different energies (from Ref. [13]). The ALICE value exceeds the RHIC one by a factor of two.

the analogous volume at RHIC and scales linearly with multiplicity. The scaling becomes worse when other centralities and, in particular, smaller collision systems are included. Violation of the scaling is clearly visible when comparing the volumes measured at the LHC in pp and Pb–Pb at the same charged-particle pseudorapidity density (Fig. 8) [14]. The three HBT radii always scale linearly with the cube root of $\langle \mathrm{d}N_{\mathrm{ch}}/\mathrm{d}\eta \rangle$ but the slope of the scaling is different for protons and heavy-ions. This indicates that the HBT radii are not driven exclusively by the final multiplicity but are also sensitive to the initial geometry of the collision.

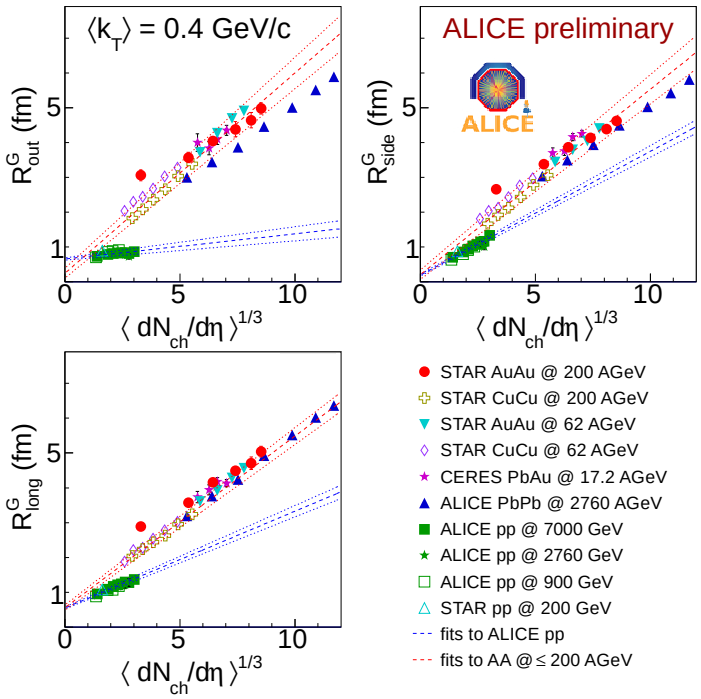

Fig. 8. Scaling of HBT radii with the charged-particle pseudorapidity density in pp and AA collisions (from Ref. [14]). The high-multiplicity pp collisions do not follow the scaling.

The collective outward motion of particles at freeze-out is the commonly accepted explanation for the fact that the HBT radii in heavy-ion collisions decrease with increasing transverse momentum. Observation of a similar p_{T} dependence in pp collisions at RHIC suggests that either this explanation has to be revised, or collective flow exists also in pp collisions. Some clarification on the subject and support to the latter statement comes from the observation that the p_{T} dependence in pp collisions develops with increasing multiplicity [15, 14]. This is shown in Fig. 9 and discussed in Ref. [14].

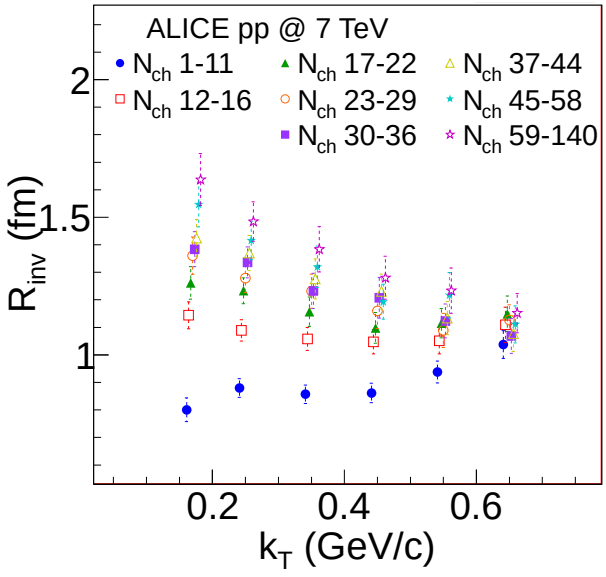

Fig. 9. Evolution of the transverse momentum dependence of HBT radii with multiplicity in pp collisions (from Ref. [14]).

5. Elliptic flow

After the RHIC experiments found that the QCD matter created in heavy-ion collisions behaved like a low-viscosity fluid, a natural question arose whether this behavior would continue at higher collision energies, or whether the system would get closer to a non-interacting gas of quarks and gluons. This question was answered by the ALICE measurement of the elliptic flow coefficient v_2 which quantifies the azimuthal anisotropy of the particle emission in non-central collisions and which, therefore, is sensitive to the early stage of the collision [16]. As is shown in Fig. 10, the elliptic flow at the LHC turned out to be higher than at RHIC and to follow the trend observed at lower energies. The v_2 increase at the LHC mostly comes from the increase in $\langle p_{\mathrm{T}} \rangle$, as the shape of the $v_2(p_{\mathrm{T}})$ dependence remains unchanged within the $\sqrt{s_{\mathrm{NN}}}$ range from 40 to 2760 GeV.

The elliptic flow coefficient of identified hadrons shows a splitting which is characteristic to the presence of transverse radial flow (Fig. 11) [17, 18]. The shape of the p_{T} dependence and the presence of the splitting are fairly well reproduced by hydrodynamics [19]. The calculation, however, underpredicts the elliptic flow of protons. This can be cured by adding hadronic rescattering [19].

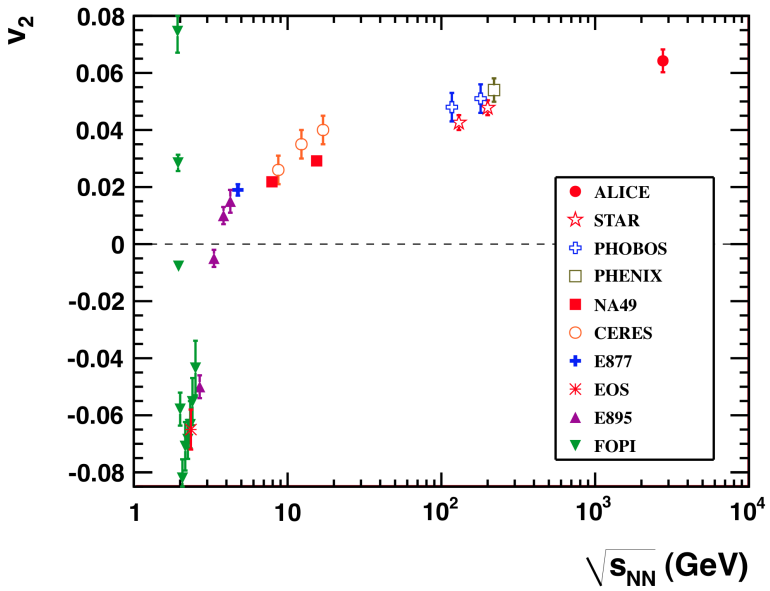

Fig. 10. Collision energy dependence of the elliptic flow (from Ref. [16]). The ALICE measurement matches the trend established at lower energies.

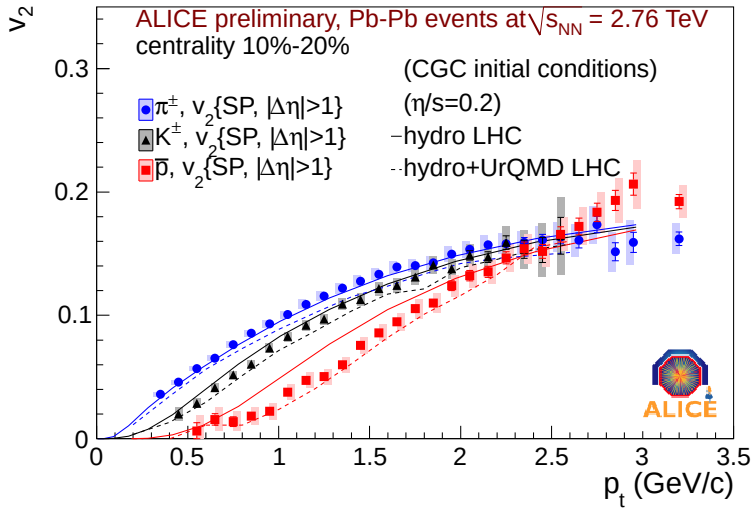

Fig. 11. Transverse momentum dependence of the elliptic flow of pions, kaons, and protons (variation of figure from Ref. [18]). The splitting is characteristic for transverse radial flow. The model description of protons can be improved by adding rescattering (red dashed line).

An important role at the LHC is played by the triangular flow. Its coefficient v_3 only weakly depends on centrality and its direction is not related to the orientation of the event plane which points to the initial energy density fluctuations as its origin. There are indications that the "Mach cone"-like azimuthal emission pattern is actually just a superposition of the elliptic and triangular collective flow [20].

6. Probing QCD matter

The parton energy loss in QCD medium manifests itself as a suppression of high-pt hadrons. Figure 12 shows the nuclear modification factor, i.e. the ratio of transverse momentum spectra to those from pp collisions, normalized to the mean overlap function $\langle T_{AA} \rangle$ of Pb–Pb collisions within the given centrality range

$$R_{AA}(p_{\rm T}) = \frac{{\rm d}^2 N_{AA}/{\rm d}\eta {\rm d}p_{\rm T}}{\langle T_{AA} \rangle \; {\rm d}^2\sigma_{\rm pp}/{\rm d}\eta {\rm d}p_{\rm T}} \; , \tag{1}$$

for charged particles in p–Pb and Pb–Pb [21]. There is no suppression of high $p_{\rm T}$ particles in p–Pb collisions. In central Pb–Pb collisions charged particles with $p_{\rm T}$ =7 GeV/c are suppressed by a factor of 7. At high $p_{\rm T}$

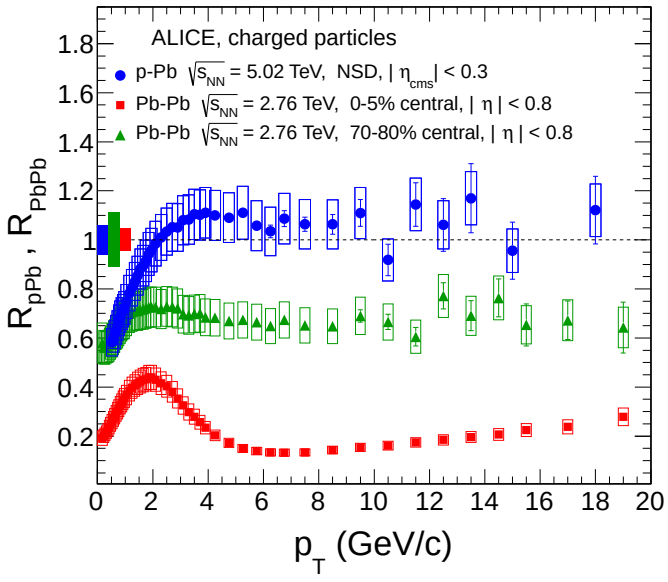

Fig. 12. Nuclear modification factor in p–Pb and Pb–Pb collisions at the LHC (from Ref. [21]).

the suppression gradually gets reduced. The suppression also weakens when going from central to peripheral collisions.

The J/ψ meson is especially sensitive to deconfined color medium [22] because it (and its parent particles) should be destroyed at high temperature according to a well defined pattern (sequential suppression) [23]. Alternative approaches envisioned these mesons being created by statistically combining c and $\bar{c}$ quarks in the deconfined medium [24] or at hadronization [25]. The two approaches, sequential suppression and statistical (re)generation, predict, respectively, suppression and enhancement of J/ψ yield when going from peripheral to central heavy-ion collisions at high energy. The J/ψ nuclear modification factor measured by ALICE in Pb–Pb collisions is shown in Fig. 13. While the measurement at forward rapidities in the muon spectrometer gives a flat dependence, the midrapidity data in the e^+e^- channel in the central barrel even suggests a slight increase. Both results significantly differ from the respective RHIC measurement and indicate a possible contribution of the (re)generation mechanism to J/ψ production.

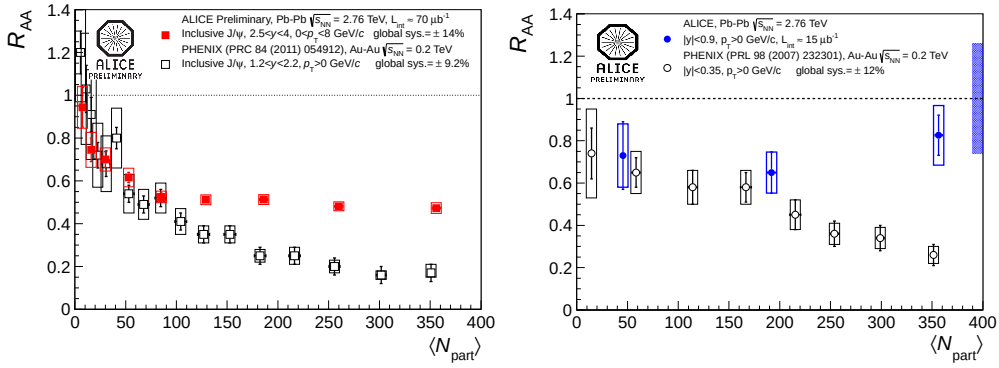

Fig. 13. Nuclear modification factor of J/ψ at forward (left) and central (right) rapidities. The J/ψ suppression at the LHC is weaker than at RHIC and indicates a possible contribution of the statistical hadronization mechanism to J/ψ yield.

Photons at central rapidities are measured in ALICE in two ways, by using calorimeters and by invariant mass analysis of e^+e^- pairs. Such pairs are produced by photons converting in the apparatus material and the distribution of their vertices provides a detailed verification of the material distribution in the detector (Fig.14).

A preliminary p_{T} spectrum of direct photons (decay photons subtracted) from central Pb–Pb collisions at the LHC [26], obtained using the photon conversion method, is shown in Fig. 15. An exponential component at low p_{T} indicates thermal emission. Its slope parameter of 299±51 MeV, if

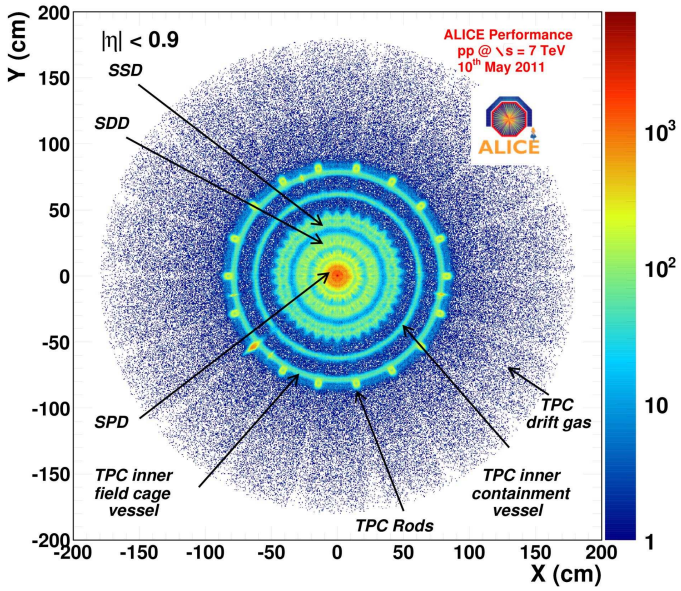

Fig. 14. Transverse distribution of $\gamma \to e^+e^-$ vertices in the ALICE central barrel, representing the material of the apparatus.

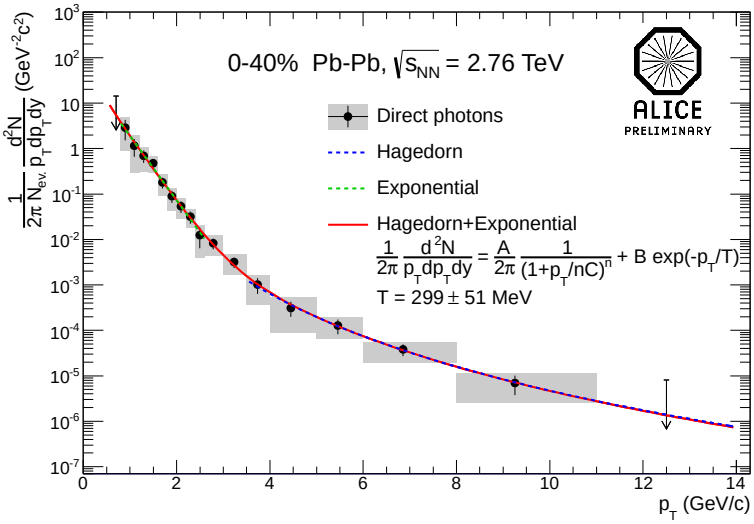

Fig. 15. Transverse momentum spectrum of direct photons in central Pb–Pb collisions at LHC (from [26]). The exponential part at low p_{T} has a slope parameter of 299±51 MeV, higher than the critical temperature $T_{\mathrm{c}} \approx 160$ MeV.

interpreted as temperature, suggests that these soft photons originate from deconfined medium.

7. Ridges

CMS reported a near-side ridge, i.e. enhanced emission of particles with similar azimuthal angles ($|\Delta\phi| \lesssim 1$) and different pseudorapidities (up to $|\Delta\eta| \simeq 4$), developing in high-multiplicity pp and p–Pb collisions [27, 28]. This ridge is reminiscent of the one that is present in heavy-ion collisions and that is associated with hydrodynamic flow. The resulting debate on the possibility of flow in small collision systems got an important contribution when ALICE found that this near-side ridge in p–Pb is accompanied by an analogous one on the away side [29] (Fig. 16). The second ridge only becomes visible when the contribution of back-to-back jet pairs is subtracted,

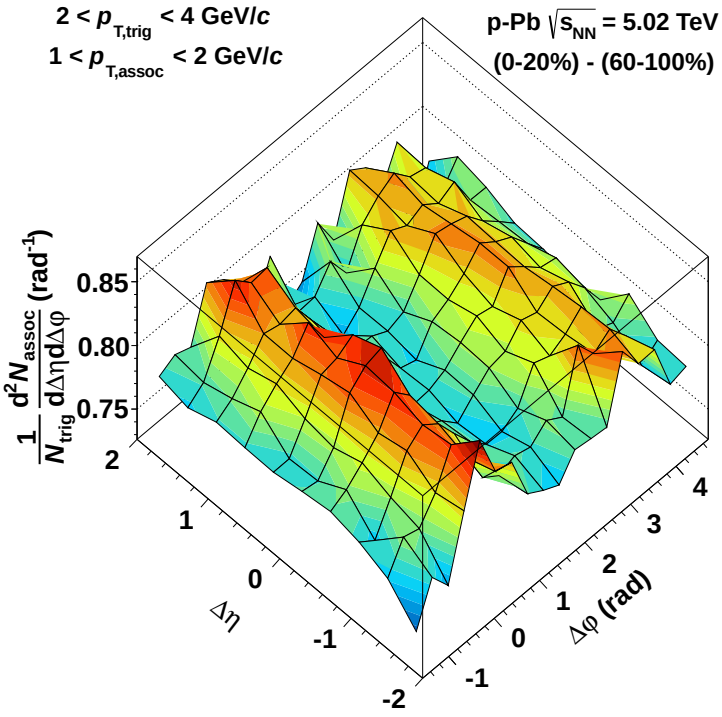

Fig. 16. Angular correlations between pairs of charged particles in p–Pb at $\sqrt{s}$ =5.02 TeV (from Ref. [29]). Shown is is the difference of distributions in high- and low-multiplicity events. The near-side ridge is accompanied by a similar ridge on the away side.

e.g. by subtracting the distributions in low-multiplicity from those in high-multiplicity collisions. Its existence supports the notion of flow in p–Pb, albeit the discussion is still ongoing.

8. Summary

During the first three years of operation of the LHC ALICE was able to inspect basically all physics observables sensitive to deconfined QCD matter. The Pb–Pb collision studies were augmented by pp and p–Pb measurements. New insights include an alternative interpretation of the angular emission pattern (flow rather than the "Mach cone"), the $p_{\rm T}$ dependence of HBT radii developing with multiplicity in pp collisions, the proton puzzle (lower than expected yield and lower elliptic flow of protons), the nuclear suppression decreasing with $p_{\rm T}$ at high transverse momentum, a hint of J/ψ production via (re)generation, and the double ridge in p–Pb.

In an introductory Student Day talk at the Goa conference in December 2010 [30] three questions to LHC were formulated that have to be answered positively before one can talk about "matter" in nuclear collisions at the LHC. Are the HBT radii larger than at RHIC? Is the spectral temperature of photons higher than at RHIC? Is J/ψ fully suppressed or, alternatively, enhanced? ALICE has answers to all these questions. The homogeneity volume is two times higher than at RHIC (Fig. 7). The photon temperature is 299±51 MeV (Fig. 15), to be compared with 221±19(stat)±19(syst) at RHIC. The J/ψ yield seems to be enhanced in central collisions, indicating possible contribution of the (re)generation mechanism (Fig. 13).

The author thanks the organizers for the invitation and for their hospitality during the meeting.

REFERENCES

[1] F. Carminati, (Ed.) *et al.* [ALICE Collaboration], J. Phys. G G **30** (2004) 1517; G. Alessandro, (Ed.) *et al.* [ALICE Collaboration], J. Phys. G G **32** (2006) 1295; K. Aamodt *et al.* [ALICE Collaboration], JINST **3** (2008) S08002.

[2] B. Abelev *et al.* [ALICE Collaboration], Phys. Rev. Lett. **110** (2013) 032301.

[3] KAamodt *et al.* [ALICE Collaboration], Eur. Phys. J. C **65** (2010) 111.

[4] K. Aamodt *et al.* [ALICE Collaboration], Eur. Phys. J. C **68** (2010) 89.

[5] B. Abelev *et al.* [ALICE Collaboration], Phys. Rev. Lett. **105** (2010) 252301.

[6] B. Abelev *et al.* [ALICE Collaboration], arXiv:1301.4361 [nucl-ex].

[7] K. Aamodt *et al.* [ALICE Collaboration], Phys. Rev. Lett. **106** (2011) 032301.

[8] B. Muller, J. Schukraft, and B. Wyslouch, Ann. Rev. Nucl. Part. Sci. **62** (2012) 361.

[9] B. Abelev *et al.* [ALICE Collaboration], arXiv:1303.0737 [hep-ex].
[10] M. Floris, J. Phys. G G **38** (2011) 124025.
[11] C. Shen, U. Heinz, P. Huovinen, and H. Song, Phys. Rev. C **84** (2011) 044903.
[12] A. Kalweit [ALICE Collaboration], Acta Phys. Polon. Supp. **5** (2012) 225.
[13] K. Aamodt *et al.* [ALICE Collaboration], Phys. Lett. B **696** (2011) 328.
[14] K. Aamodt *et al.* [ALICE Collaboration], Phys. Rev. D **84** (2011) 112004.
[15] V. Khachatryan *et al.* [CMS Collaboration], JHEP **1105** (2011) 029.
[16] K. Aamodt *et al.* [ALICE Collaboration], Phys. Rev. Lett. **105** (2010) 252302.
[17] F. Noferini [ALICE Collaboration], Acta Phys. Polon. Supp. **5** (2012) 329.
[18] M. Krzewicki [ALICE Collaboration], J. Phys. G **38** (2011) 124047.
[19] U. Heinz, C. Shen, and H. -C. Song, AIP Conf. Proc. **1441** (2012) 766.
[20] K. Aamodt *et al.* [ALICE Collaboration], Phys. Rev. Lett. **107** (2011) 032301.
[21] B. Abelev *et al.* [ALICE Collaboration], Phys. Rev. Lett. **110** (2013) 082302.
[22] T. Matsui and H. Satz, Phys. Lett. B **178** (1986) 416.
[23] S. Digal, P. Petreczky, and H. Satz, Phys. Rev. D **64** (2001) 094015.
[24] R. L. Thews, M. Schroedter, and J. Rafelski, Phys. Rev. C **63** (2001) 054905.
[25] P. Braun-Munzinger and J. Stachel, Phys. Lett. B **490** (2000) 196.
[26] M. Wilde [ALICE Collaboration], [arXiv:1210.5958 [hep-ex]].
[27] V. Khachatryan *et al.* [CMS Collaboration], JHEP **1009** (2010) 091.
[28] S. Chatrchyan *et al.* [CMS Collaboration], Phys. Lett. B **718** (2013) 795.
[29] B. Abelev *et al.* [ALICE Collaboration], arXiv:1212.2001 [nucl-ex].
[30] H. Satz, Nucl. Phys. A **862-863** (2011) 4.